Colloid Polym Sci (2007) 285:1691–1697
DOI 10.1007/s00396-007-1744-3

ORIGINAL CONTRIBUTION

Effects of ammonium chloride and heat treatment on residual formaldehyde contents of melamine-formaldehyde microcapsules

Wei Li · Jianping Wang · Xuechen Wang · Shizhen Wu · Xingxiang Zhang

Received: 25 October 2006 / Revised: 11 June 2007 / Accepted: 13 July 2007 / Published online: 8 August 2007

Abstract Microencapsulated *n*-octadecane with melamine–formaldehyde resin (MF) shell was synthesized by in situ polymerization. Ammonium chloride was used to reduce the residual formaldehyde content of microencapsulated phase change materials (microPCMs) caused by the inherent characteristics of MF. Moreover, microPCMs were heat-treated at 160 °C for 30 min. The surface morphology of the microPCMs fabricated at various microencapsulation periods was examined, and the shell thickness was measured. The effects of heat treatment on the surface morphology, residual formaldehyde content, phase change properties, and thermal stability of the microcapsules were systematically investigated. The globular surface of microcapsules fabricated at microencapsulation period of 120 min was smooth and compact with an average diameter about 2.2 μm, and the shell thickness was ranged from 30 to 70 nm. The thermal stability of heat-treated microcapsules enhanced significantly as microencapsulation period increased; in addition, the residual formaldehyde content of microcapsules decreased from 125±1 mg/kg to 19±1 mg/kg.

Keywords Microcapsule · Melamine-formaldehyde · *n*-Octadecane · Formaldehyde content · Thermal stability

Introduction

Microcapsules are microparticles with diameters in the range of 1 μm to 1 mm that consist of core materials and covering membranes. The first industrial microcapsule product, which was prepared by complex coacervation of gelatin and gum Arabic, was used for carbonless copy paper by Green and Schleicher in the 1950s [1]. From then on, microcapsules have been applied to a wide range of products such as pharmaceuticals [2–5], microencapsulated electrophoretic display system [6, 7], liquid crystals [8], and cosmetics owing mainly to their characteristics of controlled release and ability to protect them from environmental stimuli.

Phase change materials (PCMs), i.e., eutectic salts, *n*-alkanes, aliphatic polyether etc., can absorb, store, and release a large amount of latent heat over a defined temperature range while the materials change phase or state. However, the bulk PCMs are not easy to handle in practical application due to their inherent characteristics. MicroPCMs are a powder-like material and have provided an interesting alternative for using PCMs in the manufacture of thermo-regulated fibers [9–11], foams [12], building materials [13], and solar and nuclear energy storage systems [14] etc. in recent years.

A survey of literature indicates that melamine–formaldehyde (MF) [15, 16], urea–formaldehyde polymer (UF) [17, 18], urea–melamine–formaldehyde polymer (UMF) [19] and polyurethane polymer (PU) [20] are usually selected as microcapsule shell materials for the PCMs protection. Usually, the microencapsulation of PU is not easy to handle due to the fast reaction, and organic solvent such as acetone has to be employed [20]. Moreover, the microPCMs with PU shell are fragile against heat during the curing process [10]. The water resistance of UF is not as high as that of MF [21, 22]; furthermore, the MF has good seal tightness and endurance [23], acid and alkaline resistance, and fire resistance. Therefore, MF is more often used as shell material in the field of microPCMs.

W. Li · J. Wang · X. Wang · S. Wu · X. Zhang (✉)
Tianjin Municipal Key Lab of Fiber Modification and Functional Fibers, Institute of Functional Fibers,
Tianjin Polytechnic University,
Tianjin 300160, China
e-mail: zhangpolyu@yahoo.com.cn

In addition, the *n*-octadecane is selected as phase change material in the fabrication of microcapsules used in thermo-regulated fibers, as its melting and crystallization points are between the temperatures of skin and clothing. Residual formaldehyde inevitably exists after forming the shell through polymerization, such as using MF and UF resins, which, however, causes environmental and health problems. Before curing, 10 to 20 wt% of urea was used to reduce the residual formaldehyde content of microcapsules with melamine–formaldehyde resin shell [24]. We fabricated microPCMs using MF prepolymer by putting in formaldehyde once and melamine for three times (Li et al., submitted). The residual formaldehyde content of these microcapsules is 68±1 mg/kg, although their application is limited to some extent. There is, however, still little information available on fabrication of microcapsules with low formaldehyde content. MF shell microPCMs with low residual formaldehyde content were synthesized by adding ammonium chloride during the microencapsulation process in this study and then heat-treated at 160 °C to decrease the residual formaldehyde content further. The surface morphology and the dispersibility of the microcapsules were examined. The effects of heat treating on the residual formaldehyde content, thermal properties, and thermal stability of microPCMs were also systematically investigated.

Experimental

Materials

Melamine (98 wt%, Tianjin Resins Material Factory) and formaldehyde (37 wt% aqueous, A.R., Tianjin Chemical Reagent Factory) were used as monomers; *n*-octadecane (purity 99 wt%, Union Lab Supplies, Hong Kong) was used as core material. Anionic surfactant, TA (styrene–maleic anhydride copolymer, 19 wt% aqueous solution, Shanghai Leather Chemical Works) was employed as an emulsifier. Triethanolamine (95 wt%), acetic acid (36 wt%), and sodium hydroxide (A.R.), all purchased from Tianjin Chemical Regents, were used as pH regulators. Ammonium chloride (A.R.) was obtained from Tianjin Chemical Regents 3rd Inc. Epoxy resin (model 711 and 618) was purchased from Tianjin Jindong Chemical Plant.

Preparation of microcapsules

TA (13.0 g) was dispersed in 200-ml of distilled water, and the resultant micelles were heated to 65 °C. The oil phase, *n*-octadecane, was added to the micelles slowly, and the mixture was emulsified mechanically with a stirring speed of 8,000 rpm for 90 min to form an oil-in-water emulsion. The pre-polymerization was carried out in a 250-ml three-necked round-bottomed flask equipped with a mechanical stirrer. Formaldehyde (14.0-ml), melamine (7.0 g), and distilled water (15.0-ml) were added to the flask. The pH of the mixture was regulated to about 8.5 with triethanolamine. The prepolymer was prepared at 70 °C with a stirring speed of 250 rpm until the mixture became transparent. The emulsion was shifted to a 500-ml three-necked round-bottomed flask after the pH was regulated to approximately 4.5. Then, the prepolymer was dropped at a rate of approximately 0.8 ml/min into the emulsion system to start in situ polymerization at 70 °C with a stirring speed of 600 rpm. The suspension was continuously stirred for 10 min after the prepolymer was totally added. Then, 5.4 g of ammonium chloride was added into the system to remove the residual formaldehyde (as shown in Eq. 1) [25] and the reaction continued for different periods: 30, 60, 90, and 120 min, respectively. The resultant microcapsules were filtered and washed with 30 wt% ethanol solution at approximately 50 °C twice to remove remaining reactants and TA and then dried in the air.

$$4NH_4Cl + 6CH_2O \rightarrow (CH_2)_6N_4 + 6H_2O + 4HCl \qquad (1)$$

The dried microcapsules were then heat-treated in an oven at 160 °C for 30 min.

Preparation of shell polymer powder

The polymer shell powder was prepared by adjusting the prepolymer solution to pH 9 with 50 wt% triethanolamine solution. Then, the mixture of polymer and water was filtered, and the wet cake was dried in an oven at 100 °C for 8 h to remove the water.

Microcapsule characterization

The morphology and dispersibility of microcapsules were obtained using scanning electronic microscope (SEM, Philips XL30). A drop of the microcapsule suspension was dripped on a stainless steel SEM stub and air-dried overnight. The samples were gold-coated.

The diameters of the microcapsules were measured on the SEM photos. More than 200 microcapsules were counted. The diameter distribution was processed with Origin 7.5 Professional.

The dry microcapsules were added into a liquid epoxy resin containing curing agent. Then, the mixture was stirred fully and cured for 6 h in a 4×1×0.5-cm model made of paper. The solidified mixture was broken at room temperature and then gold-coated. The thickness of the shell was measured from the SEM images of cross-section of the microcapsules.

Fourier transform infrared spectroscopy (FTIR) spectra of *n*-octadecane, microcapsules, heat-treated microcapsules, and shell material were obtained using a spectrophotometer (Bruker Uecior 22, wave numbers 400~4,000 cm^{-1}) at room temperature.

The thermal properties of microcapsules and *n*-octadecane were investigated using differential scanning calorimetry (DSC, Perkin-Elmer, DSC7) in the range of 0 to 80 °C at a heating or cooling rate of ±10 °C/min under a nitrogen atmosphere.

The thermal stability of microcapsules, heat-treated microcapsules, and *n*–octadecane was obtained using thermogravimetric analysis (TGA, Netzsch STA 409 PC/PG TG-DT) at a scanning rate of 10 °C/min in the temperature range of 30~600 °C, and the atmosphere was nitrogen.

Measurement of residual formaldehyde content of the microcapsules

The formaldehyde can react with phenolphthalein reagent to form azine, and the azine can be oxidized by ferrate ion in an acidic solution; then, a blue-green compound can be obtained [26]. The intensity of the color is proportional to the quantity of formaldehyde present. This indicates that the residual formaldehyde contents in both the microcapsules and heat-treated microcapsules can be determined with phenolphthalein reagent (C_6H_4SN (CH_3) $CNNH_2$·HCl, MBTH).

Briefly, approximately 150 mg of dried microcapsules was wrapped with a filter paper and immersed in 100-ml water for 1 h. Then, the wrapped microcapsules were removed from solution. An extraction solution was obtained. Phenolphthalein solution (5.0 ml 0.05 g/l) and ferrate ion (0.4 ml 1.0 wt%) solution were added in 1.0-ml extraction solution for coloration. The absorbance at wavelength of 630 nm of this solution was measured using a spectral photometer (Beijing Rayleigh Analytical Instrument, VIS-7220) at room temperature; then, the concentration of the formaldehyde solution was obtained from the formaldehyde calibration curve (Fig. 1). Finally, the residual formaldehyde content of microPCMs was calculated according to the volume and concentration of the formaldehyde solution and mass of microPCMs.

Calculation of *n*-octadecane content in the microcapsules

The specific heat of *n*-octadecane was a constant in the measured temperature range. We suppose that *n*-octadecane totally crystallized in the microcapsules. The content of *n*-octadecane in the microcapsules can be estimated according to the measured enthalpy [16, 19]:

$$n-\text{octadecane content} = \frac{|\Delta H_c|}{|\Delta H_{co}|} \times 100\% \quad (2)$$

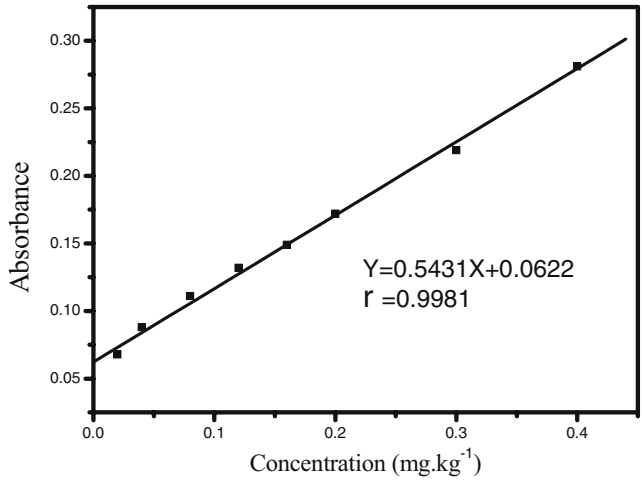

Fig. 1 Calibration curve of formaldehyde concentration

where, $|\Delta H_c|$ is the enthalpy of microcapsules (J/g) and $|\Delta H_{co}|$ is the enthalpy of *n*-octadecane, here, it is 243 J/g (DSC enthalpy of crystallization).

Calculation of shell thickness of microcapsules

We suppose that the microcapsule is a round globule as shown in Fig. 2. The mass of *n*-octadecane is [27, 28],

$$\frac{4}{3} \bullet \pi \bullet r^3 \bullet \rho_C = M_C \quad (3)$$

where, M_c is mass of *n*-octadecane; r is the radius of the core of the microcapsule; ρ_c is the density of *n*-octadecane (here, it is 0.775 g/cm^{-3}).

$$\frac{4}{3} \bullet \pi \bullet R^3 \bullet \rho_S - \frac{4}{3} \bullet \pi \bullet r^3 \bullet \rho_S = M_S \quad (4)$$

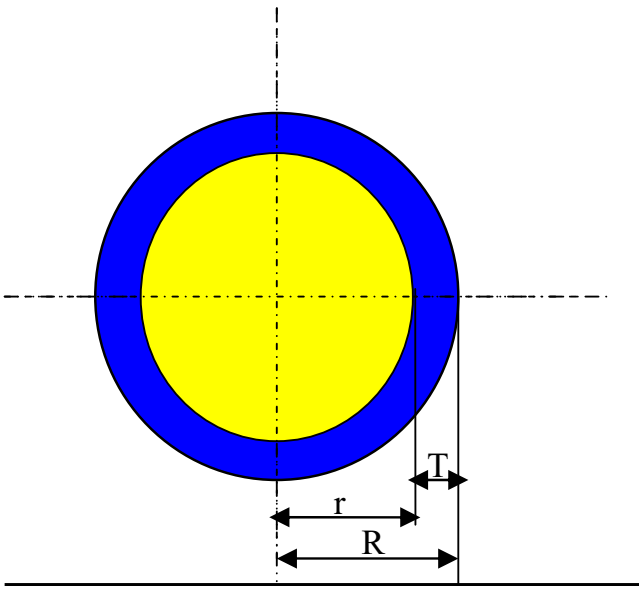

Fig. 2 Schematic diagram of microcapsules

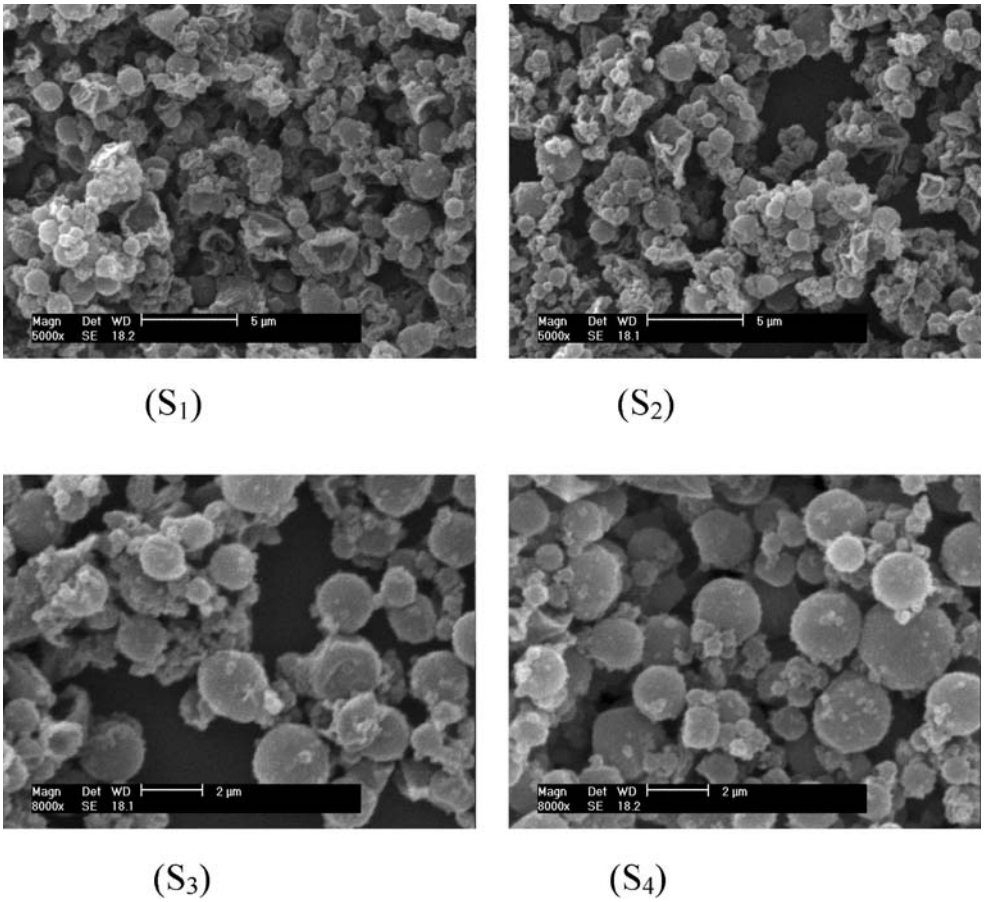

Fig. 3 SEM micrographs of microPCMs synthesized at various microencapsulation periods: (S_1) 30 min; (S_2) 60 min; (S_3) 90 min; (S_4) 120 min

where M_s is the mass of MF shell; R is the radius of the microcapsule; ρ_s is the density of MF resin (here, it is 1.43 g/cm^{-3}).

$$P = \frac{M_C}{M_C + M_S} \times 100\% \tag{5}$$

where P is the content of *n*-octadecane.

$$T = R - r \tag{6}$$

where T is the thickness of MF shells.

$$T = R \bullet \left(1 - \sqrt[3]{\frac{P \bullet \rho_S}{\rho_C - P \bullet \rho_C + P \bullet \rho_S}}\right) \tag{7}$$

Results and discussion

Morphology of microPCMs synthesized at various microencapsulation periods

SEM micrographs of microcapsules prepared at various microencapsulation periods are shown in Fig. 3. Only a few round globular microcapsules were observed for samples S_1 and S_2. Most of the microcapsules shrank due to the incomplete encapsulation of *n*-octadecane. By contrast, most of the microcapsules were round globule for samples S_3 and S_4. The microencapsulation efficiency increased significantly, and the agglomerated microcapsules decreased with the increase of microencapsulation periods

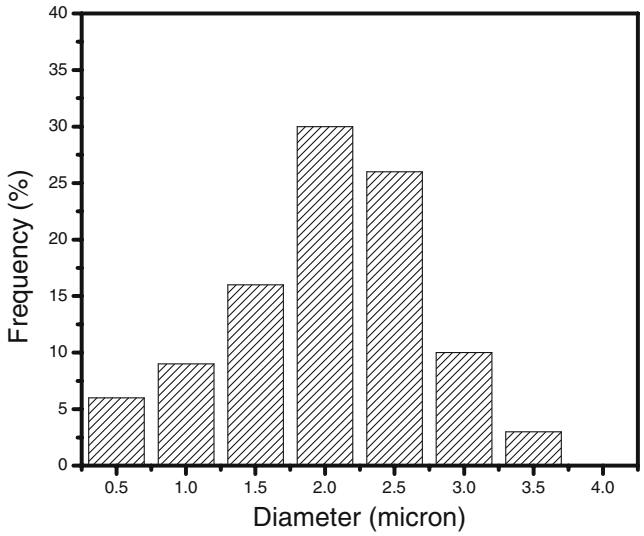

Fig. 4 Diameter distribution of S_4 microcapsules

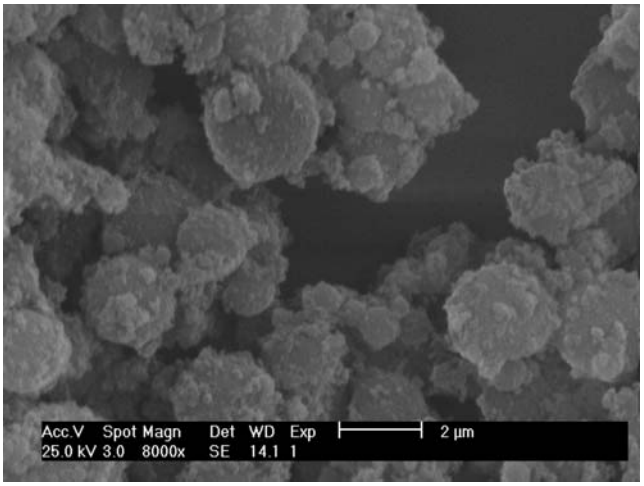

Fig. 5 SEM micrographs of S_4 heat-treated at 160 °C for 30 min

when the dropping rate and temperature elevating rate were kept constant. The globular surface became smooth and compact with the microencapsulation periods prolonged. The low microencapsulation efficiency between the S_1 and S_2 microcapsule was mainly attributed to the fact that there was no enough time for shell condensation reaction, and the shell strength could not endure the treatment such as washing.

Most of the S_4 microcapsules were globules with an average diameter of about 2.2 μm. The diameter distribution is presented in Fig. 4.

Figure 5 shows SEM micrographs of S_4 microcapsules heat-treated at 160 °C for 30 min. The smoothness of the surface decreased slightly; however, most of the microcapsules were intact.

Shell thickness of microcapsules

As presented in Fig. 6, the microcapsules scattered in epoxy resin separately. The cavities that were caused by the core falling off were observed after the microcapsules in the epoxy resin were broken. The fragment of shell material conglutinated with the resin kept shape, however. From the SEM micrographs in Fig. 7b, the shell thickness was measured to be 30–70 nm. The calculated shell thickness, which was approximately 86 nm, is a little larger than the measured value.

FTIR spectra

The FTIR spectra of *n*-octadecane, polymer shell, microencapsulated *n*-octadecane, and microcapsules heat-treated at 160 °C for 30 min are presented in Fig. 7. The multiple strong absorption peaks located at approximately 2,848–2,916 cm^{-1} and 717 cm^{-1} in the spectra of *n*-octadecane, and the microcapsules were associated with the aliphatic C–H stretching vibration and the in-plane rocking vibration of the CH_2 group, respectively. None of these specific peaks were observed in the spectrum of the polymer shell, however. These characterized peaks observed in the spectra of the microcapsules indicated the *n*-octadecane being encapsulated as core successfully.

Thermal properties of microcapsules

The DSC cooling curves of S_4, heat-treated S_4, and *n*-octadecane are shown in Fig. 8. There were two peaks visible from the DSC cooling curves of both S_4 and heat-treated S_4, marked as alpha and beta, respectively. While only one peak, alpha, was visible from the DSC cooling curve of *n*-octadecane, which was attributed to the heterogeneous nucleated liquid–crystal transition. The exothermic peak alpha on both S_4 and heat-treated S_4 corresponded to the heterogeneous nucleated liquid-rotator transition [19], and it is highly likely that the homogeneous nucleated liquid–rotator and rotator–crystal transitions were captured in the peak beta and its shoulder. Rotator phase is a weakly ordered crystallization phase occurring in equilibrium at temperature between the liquid phase and the melt. Peak beta, the largest peak, was attributed to homogeneous nucleated liquid–crystal transition [19].

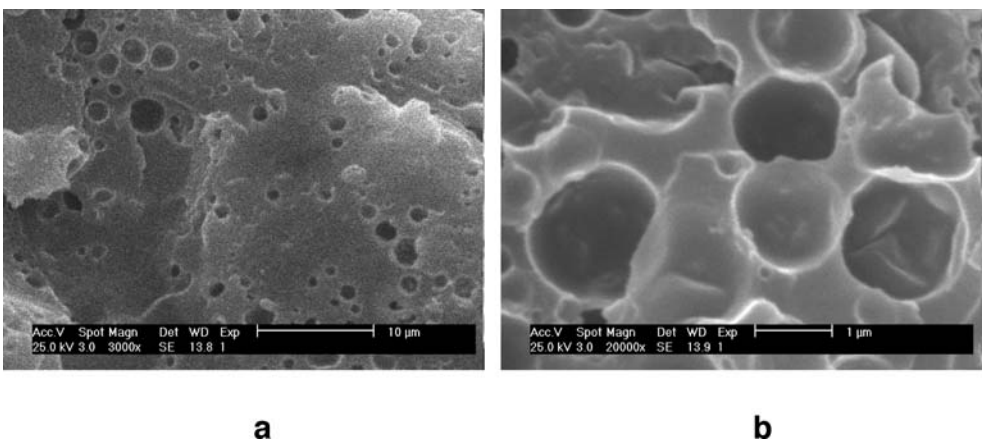

Fig. 6 SEM micrographs of cross-section of S_4 in epoxy resin: **a** ×3,000; **b** ×20,000

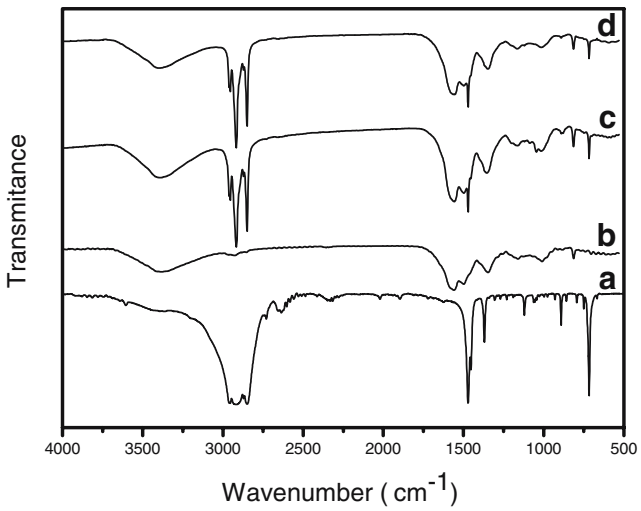

Fig. 7 FTIR spectra of *n*-octadecane, polymer shell, and microencapsulated *n*-octadecane: (*A*) *n*-octadecane, (*B*) polymer shell, (*C*) microencapsulated *n*-octadecane, (*D*) microcapsules heat-treated at 160 °C for 30 min

The phase change properties of *n*-octadecane, S_4, and heat-treated S_4 are listed in Table 1. The measured content of *n*-octadecane in S_4 was slightly higher than the calculated value according to the ratio of raw materials. The difference was caused by the elimination of water and formaldehyde from the reaction of hydroxymethyl groups and the partial removal of emulsifier during the wash of microcapsules (Li et al., submitted). The *n*-octadecane was totally encapsulated in S_4 microcapsules. The contents of *n*-octadecane in S_4 decreased from 66.3 to 58.0 wt% after heat treatment at 160 °C for 30 min. This is possibly caused by the evaporation of *n*-octadecane adhered on the surface and diffused from a few delicate microcapsules during the heat treatment [29]. The diffusion of *n*-octadecane through the microcapsule shell in the heat treatment process is the major mode by which the capsules lose the core materials. As shown in Fig. 6, the diffused *n*-octadecane was adhered to the surface after solidification that led to the rough surface of heat-treated microcapsules [30].

Table 1 Phase change properties of *n*-octadecane and S_4 and heat-treated S_4

PCM/ microPCMs	T_c (°C)		ΔH_c (J/g)	Measured content of *n*-octadecane (wt%)	Calculated content of *n*-octadecane (wt%)
	Alpha	Beta			
n-Octadecane	27.1± 0.5		243±5	–	–
S_4	29.2± 0.5	14.8± 0.5	161±5	66.3±0.02	63
Heat-treated S_4	27.7± 0.5	15.8± 0.5	141±5	58.0±0.02	63

T_c Peak temperature on DSC cooling curve, ΔH_c enthalpy on DSC cooling curve (sum of peak areas of alpha and beta)

Thermal stability of microPCMs

TGA curves of heat-treated microcapsules, microencapsulated *n*-octadecane, and *n*-octadecane are presented in Fig. 9. The weight of *n*-octadecane and microcapsules decreased with the temperature increasing. The *n*-octadecane began to lose weight at nearly 180 °C and lost weight completely at approximately 270 °C. The boiling point of *n*-octadecane is 308 °C [31]; however, *n*-octadecane evaporated before boiling. By contrast, the weight loss rate of sample S_4 and heat-treated S_4 was obviously lower than that of *n*-octadecane bulk. The MF shell protected *n*-octadecane from losing weight quickly.

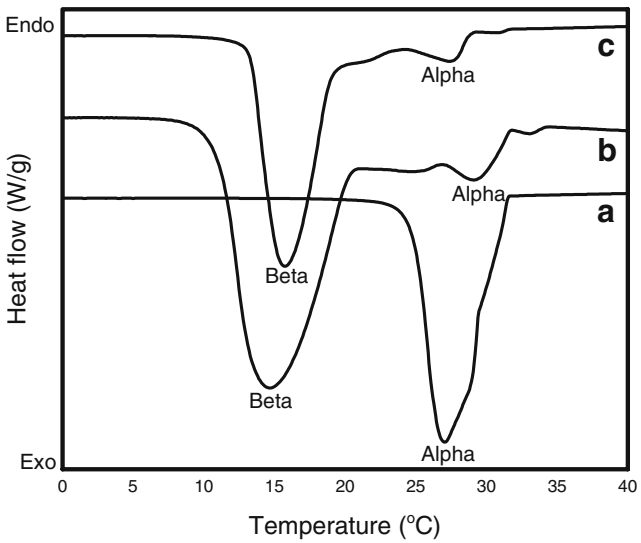

Fig. 8 DSC curves of *n*-octadecane and MicroPCMs: (*A*) *n*-octadecane, (*B*) S_4, (*C*) S_4 heat-treated at 160 °C for 30 min

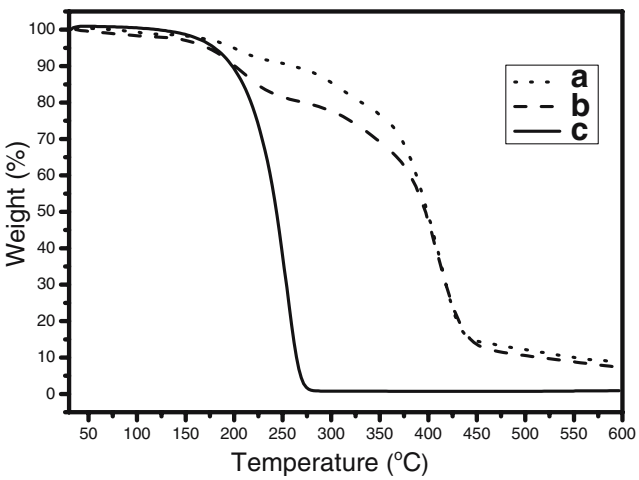

Fig. 9 TGA curves of heat-treated microcapsules, microencapsulated *n*-octadecane and *n*-octadecane: (*A*) heat-treated S_4, (*B*) S_4, (*C*) *n*-octadecane

Previous research shows that [30] the weight loss temperature is enhanced as the heat-treated temperature increases from 120 to 160 °C. This may be explained by the cross-linking formed during the heat treatment process with the elimination of water and formaldehyde from the reaction of hydroxymethyl groups. The formation of "methylene" cross-links strengthens the shell and reduces the content of volatile component. The preferable heat treatment temperature is 160 °C, which is equivalent to the molding temperature of melamine–formaldehyde resin. The thermal stability in the range of 150–380 °C of S_4 heat-treated at 160 °C was higher than that of S_4. The improvement of thermal stability of heat-treated microcapsules was not totally due to the evaporation of water, formaldehyde, or the decomposition of emulsifier, as the evaporation or decomposition of these materials would increase the enthalpy of microPCMs. However, the enthalpy of heat-treated microcapsules was lower than that of untreated, as shown in Table 1. It is also probable that some of the delicate microcapsules were destroyed by the heat treatment at 160 °C [30], and the MF shell was left. If appropriate expansion space were added inside the MicroPCMs, the highest thermal stable temperature would be as high as 289 °C [29].

Residual formaldehyde content of microPCMs

Formaldehyde calibration curve and equation can be obtained using absorbance values of different formaldehyde concentration. According to the formaldehyde calibration curve and equation above, the residual formaldehyde content of S_4 microcapsules was 125±1 mg/kg, while the formaldehyde content of the heat-treated microcapsules was 19±1 mg/kg. The heat-treated microPCMs could not only be used at higher temperatures but also be used with lower residual formaldehyde content. The added ammonium chloride reacted with the residual formaldehyde to form a water-soluble compound $(CH_2)_6N_4$ [25]; further, the heat-treating at 160 °C for 30 min could reduce the formaldehyde content. By contrast, the residual formaldehyde content of the microPCMs prepared by putting in formaldehyde once and melamine for three times was 68±1 mg/kg (Li et al., submitted). The microcapsules with low free formaldehyde content are more environmental friendly, and therefore, have promising application prospects.

Conclusions

MicroPCMs with low residual formaldehyde content have been synthesized by adding ammonium chloride during the microencapsulation and then heat-treating; the best microencapsulation period was 120 min at least. The globular surface of microcapsules was smooth and compact, and the dispersibility was good. The diameter of microcapsules ranged from 0.5 to 3.5 μm, with an average diameter of about 2.2 μm. The shell thickness was in the range of 30~70 nm. The thermal stability in the range of 150–380 °C of heat-treated microcapsules was enhanced. In addition, the residual formaldehyde content of microcapsules was decreased from 125±1 mg/kg to 19±1 mg/kg.

Acknowledgments The authors thank the National Natural Science Foundation of China (50073015) and Specialized Research Fund for the Doctoral Program of Higher Education (20050058004) for financial supports.

References

1. Green BK, Schleicher L (1957) USP 2800457
2. Park SJ, Kim SH (2004) J Colloid Intern Sci 271:336
3. Xing FB, Cheng GX, Yang BX et al (2004) J Appl Polym Sci 91:2669
4. Chu LY, Liang YJ, Chen WM et al (2004) Colloid Surf B Biointerface 37:9
5. Meng FT, Ma GH, Liu YD et al (2004) Colloid Surf B Biointerface 33:177
6. Comiskey B, Albert JD, Yoshizawa H et al (1998) Nature 394:253
7. Chen Y, Au J, Kazlas P et al (2003) Nature 423:136
8. Ju HK, Kim JW, Han SH et al (2002) Colloid Polym Sci 280:879
9. Zhang XX, Wang XC, Tao XM et al (2005) J Mater Sci 40:3729
10. Kim J, Cho G (2002) Textile Res J 12:1093
11. Bryant YG, Colvin DP (1992) New Text-new Tech, Techtextile Symposium, Frankfurt, Germany, 1
12. Colvin DP (1999) Adv Heat Mass Transfer Biotech ASME HTD-363/BED-44:199
13. Su JF, Wang LX, Ren L (2005) J Appl Polym Sci 97:1755
14. Chaurasia PBL (2000) Energy Convers Manag 41:1569
15. Yamagishi Y, Takeuchi H, Pyatenko AT et al (1999) AIChE J 45:696
16. Zhang XX, Fan YF, Tao XM et al (2004) Mater Chem Phys 88:300
17. Charunyakorn P, Sengupta S, Roy SK (1991) Int J Heat Mass Transfer 34:819
18. Brown RC, Rasberry JD, Overmann SP (1998) Powder Tech 98:217
19. Zhang XX, Fan YF, Tao XM et al (2005) J Colloid Interface Sci 281:299
20. Cho JS, Kwon A, Cho CG (2002) Colloid Polym Sci 280:260
21. Lee YH, Kim CA, Jang WH et al (2001) Polymer 42:8277
22. Zanetti M, Pizzi A (2003) J Appl Polym Sci 88:287
23. Fan YF, Zhang XX, Wu SZ et al (2005) Thermochimica Acta 429:25
24. Biastoch R, Frank G (2001) USP 6224795
25. Ge YR, Feng W (2003) China Surfactant Detergent & Cosmetics (Chinese) 33:337
26. Yang MG, Wang TR, Jin YF (2005) Chinese Journal of Current Practical Medicine (Chinese) 14:80
27. Ren XL, Wang LX, Ren L, Su JF (2005) J Funct Mat (Chinese) 11 (36):1722
28. Song ZH, Zhang ZY, Dong ZZ, Wu SZ, Wang SG (2006) J Tianjin Polytechnic University (Chinese) 25(3):5
29. Zhang XX, Tao XM, Yick KL, Fan YF (2005) J Appl Polym Sci 97:390
30. Zhang XX, Tao XM, Yick KL (2004) Colloid Polym Sci 282:330
31. Freund M, Csikós R, Keszthelyi S, Mózes GY (1982) Paraffin products, properties, technologies, applications. Elsevier Scientific, Amsterdam, pp 14–15